Electronic Supplementary Information (ESI)

Tunable Optical Absorption in Lead-Free Perovskite-Like Hybrid by Iodide Management

Bo Kou,[a,b] Weichuan Zhang,[b] Chengmin Ji,[b] Zhenyue Wu,[b] Shuhua Zhang,[*a], Xitao Liu,[*b,c], and Junhua Luo[*b]

[a] College of Chemistry and Bioengineering (Guangxi Key Laboratory of Electrochemical and Magnetochemical Functional Materials), Guilin University of Technology, Guilin, Guangxi, 541004, P. R. China,

[b] State Key Laboratory of Structural Chemistry, Fujian Institute of Research on the Structure of Matter, Chinese Academy of Sciences, Fuzhou, 350002, China

[c] State Key Laboratory of Crystal Materials, Shandong University, Jinan, 250100, China.

Experimental section

Materials

A reaction mixture, containing Bis-(2-dimethylaminoethyl) ether (1.60 g, 10 mmol) and Bi_2O_3(1.16 g, 2.5 mmol) in 30 mL of HI (47%) solution, was slowly evaporated at room temperature. After several days, red crystal powder of (Bis-(2-dimethylaminoethyl) ether)Bi_2I_8 **(1)** was obtained. For the growth of (Bis-(2-dimethylaminoethyl) ether)$_2IBi_2I_9$ **(2)** crystals, add 1 mL hypophosphorous acid to the solution of **1**, and slowly evaporates at room temperature. About two weeks later, red flake crystals were obtained. For the growth of (Bis-(2-dimethylaminoethyl)ether)$_3I_3Bi_3I_{14}$ **(3)** crystals, **1** was redissolved in an oxidized hydroiodic acid solution, and black bulk crystals were obtained after slow evaporation in a few days.

Powder X-Ray Diffraction Analysis

MiniFlex Ⅱ Powder X-Ray Diffractometer (PXRD) was used to check the phase purity of desired compounds. The experimental PXRD patterns were recorded in the 2theta (2θ) range of 5°-50° with a step size of 5°. The experimental PXRD patterns obtained at room temperature match fairly well with the calculated data based on the single-crystal structure, which solidly confirm the purity of the as-grown crystals of **1**, **2** and **3**.

Structure Determination

Single crystal X-ray diffraction (SCXRD) was performed on D-8 diffractometer by using Mo-Kα radiation (λ=0.71073 Å). Intensity data acquisition, data reduction and cell refinement were performed using the CrysAlisPro program. The structures of all desired compounds were solved by direct methods and refinements were made by the least-squares program. Table S1 summarizes the detailed information of crystal parameters, structure refinement and data collection. The selected bond lengths and angles are shown in table S2-S4.

Ultraviolet-visible (UV-vis) Absorption Spectrum

UV-vis diffuse reflectance spectroscopy of desired materials were performed at room temperature on Perkin-Elmer Lambda 900 UV-Vis spectrophotometer in a variable wavelength range between 200 to 1000nm. The $BaSO_4$ was used as the 100% reflectance reference, and the powdered crystals were used for the measurements.

Near the cut-off of the optical transmission, the band gap, the absorption and the wave frequency obey the equation: $\alpha hv = A(hv - Eg)^{n/2}$

where α, v, A, and Eg are absorption coefficient, light frequency, proportionality constant, and band gap, respectively. In the equation, n decides the characteristics of the transition in a semiconductor (n=1, indirect absorption; n=4, indirect absorption). The values of n and Eg were determined by the following steps: first, plot ln(αhv) vs ln(hv - Eg) using the approximate Eg value, and then determine the value of n with the slope of the straight line near the band edge; second, plot $(\alpha hv)^{1/n}$ vs hv and then obtain the band gap Eg by extrapolating the straight line to the hv axis intercept.

First-principles calculations

First-principles DFT calculations were performed by using the plane-wave pseudopotential method implemented in the CASTEP package. The exchange-correlation energies were described by using the Perdew–Burke–Ernzerhof for solids (PBEsol) functional within the generalized gradient approximation (GGA). The normal-conserving pseudopotential (NCP) with a high kinetic cutoff energy of 750 eV and a 2×2×1 Monkhorst–Pack grid were chosen to achieve energy convergence during the self-consistent calculations. The following orbital electrons were explicitly treated as valence electrons: Bi, $5d^{10}6s^26p^3$; I, $5s^25p^5$; C,$2s^22p^2$; N, $2s^22p^3$; O, $2s^22p^4$ and H, $1s^1$.

Photoelectric Responses and Conductivity.

Photoelectric responses of **2** and **3** were tested on a current meter (Keithley6517B) by using lateral two-probe devices based on crystal samples under the wavelengths of 420 nm, and the photoelectric activity under simulated sunlight illumination was also measured. The I−V curves were also tested at a fixed voltage (10 V) at different temperatures; thus, their variable-temperature conductivities were calculated to range from 320 to 420 K.

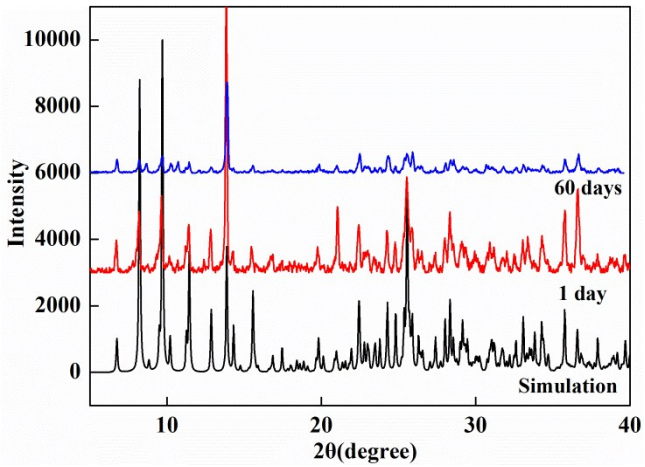

Figure S1. X-ray diffraction patterns for **1**.

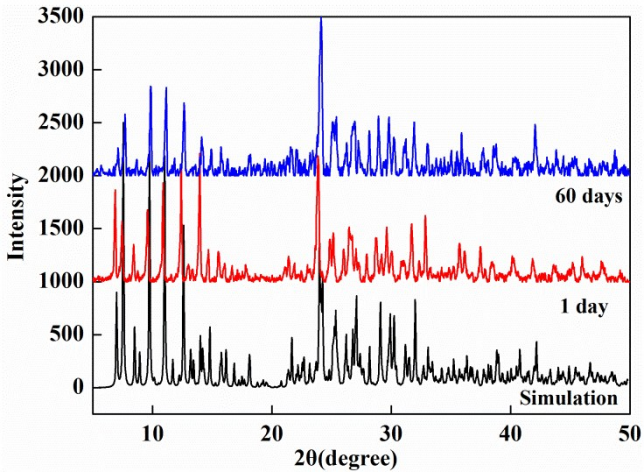

Figure S2. X-ray diffraction patterns for **2**.

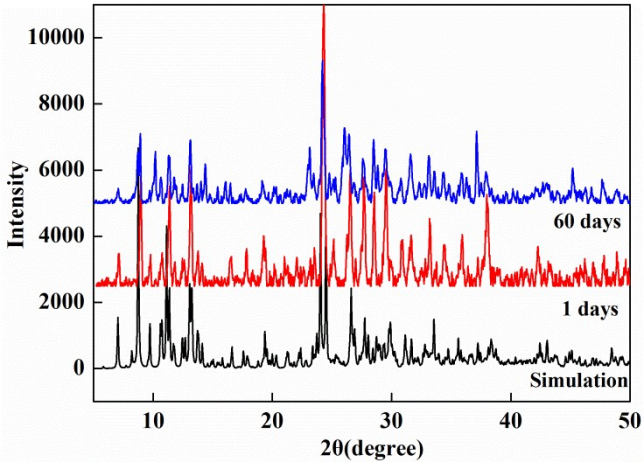

Figure S3. X-ray diffraction patterns for **3**.

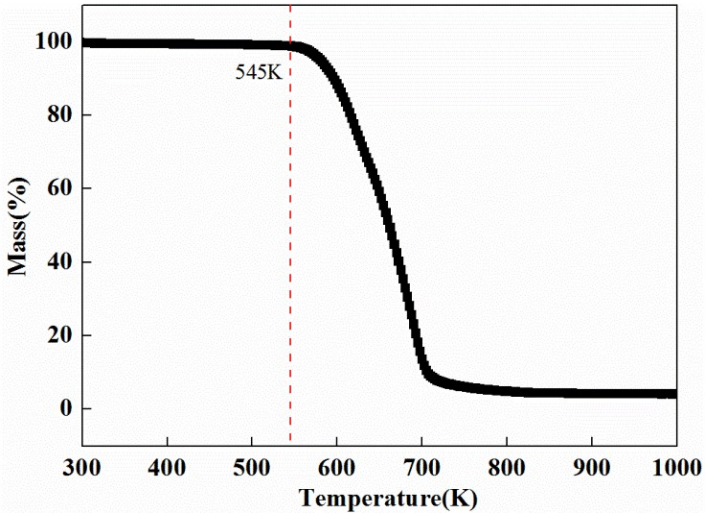

Figure S4. Thermal stability of **1** measured by TGA method, showing a high thermal stability up to 545K.

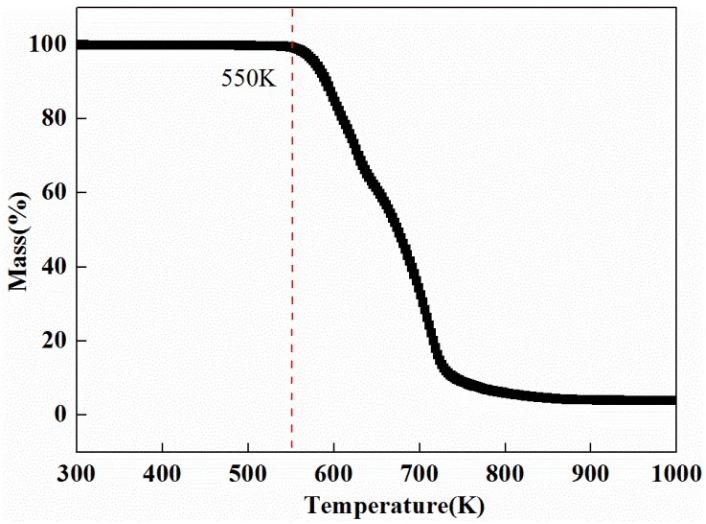

Figure S5. Thermal stability of **2** measured by TGA method, showing a high thermal stability up to 550K.

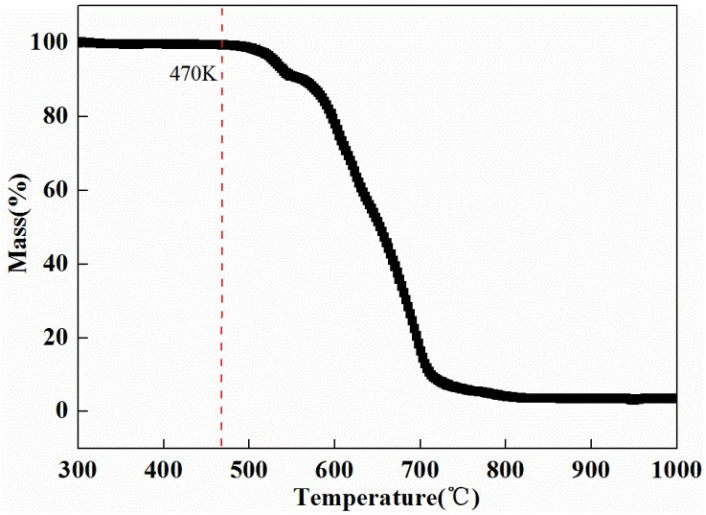

Figure S6. Thermal stability of **3** measured by TGA method, showing a high thermal stability up to 470K.

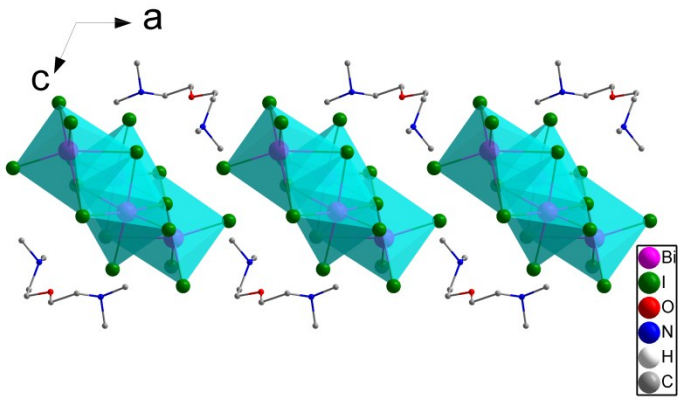

Figure S7. The packing diagram of **1**. Hydrogen atoms were omitted for clarity.

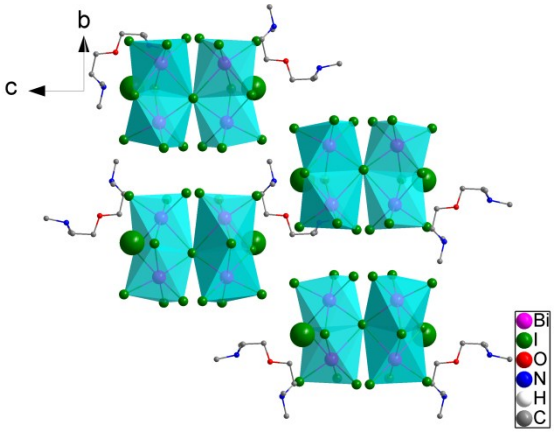

Figure S8. The packing diagram of **2**. Hydrogen atoms were omitted for clarity. The big green balls represent free iodide ions.

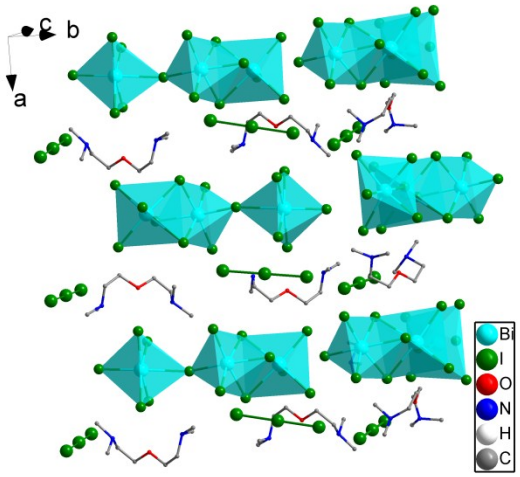

Figure S9. The packing diagram of **3**. Hydrogen atoms were omitted for clarity.

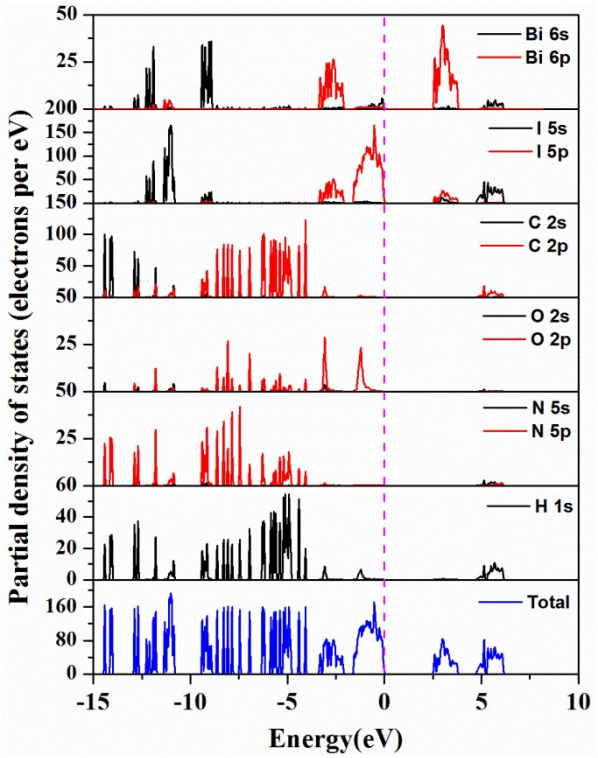

Figure S10. The PDOS of **1**.

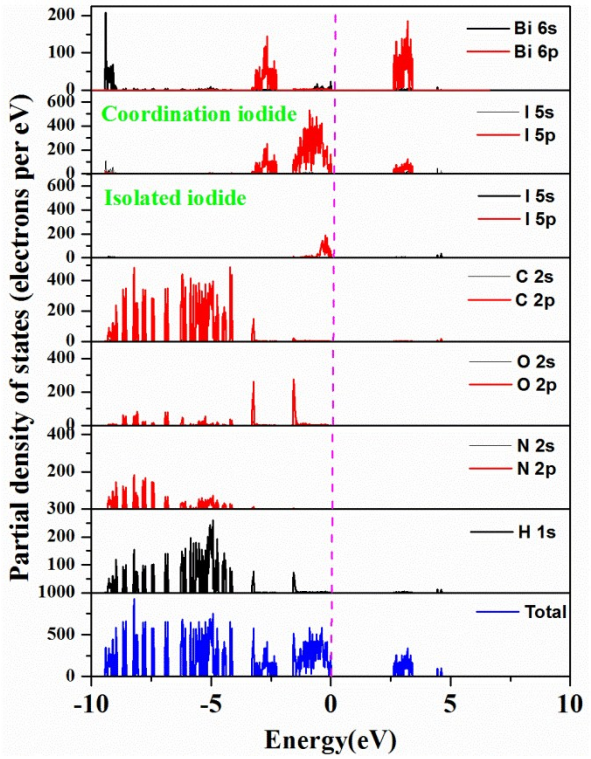

Figure S11. The PDOS of **2**.

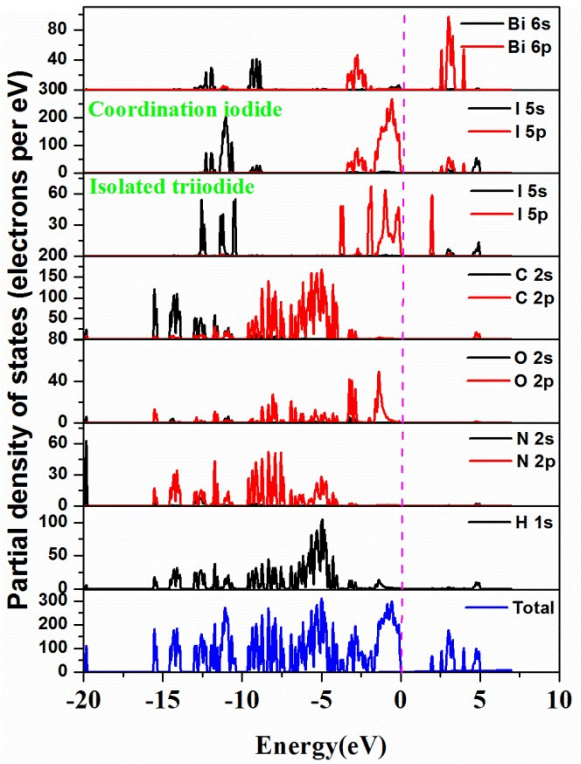

Figure S12. The PDOS of **3**.

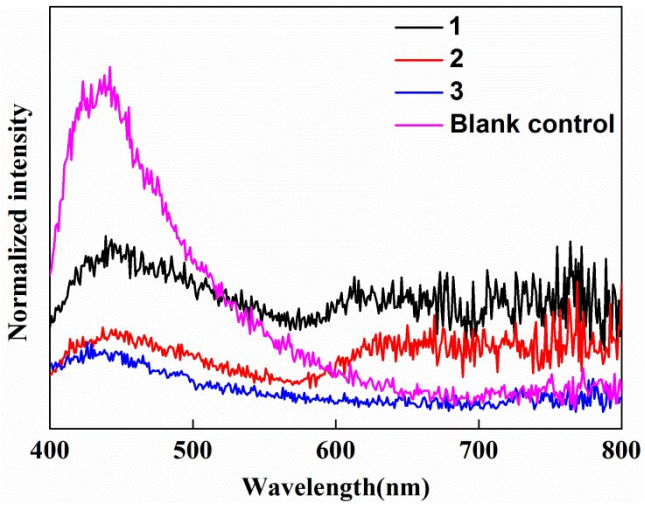

Figure S13: Photoluminescence spectra for **1**, **2** and **3**.

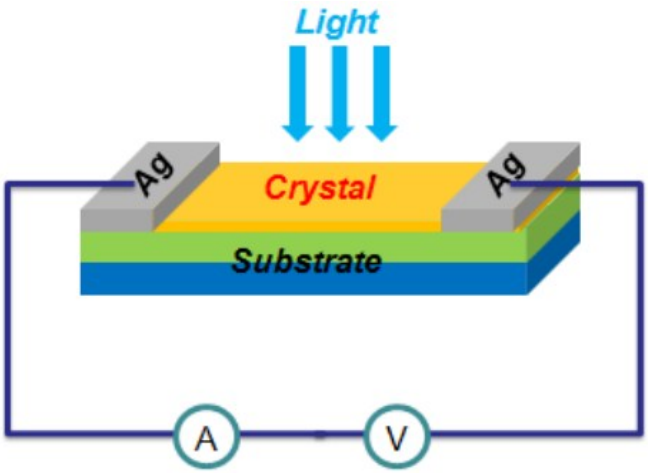

Figure S14. Schematic diagram of photoconductive device based on single crystal.

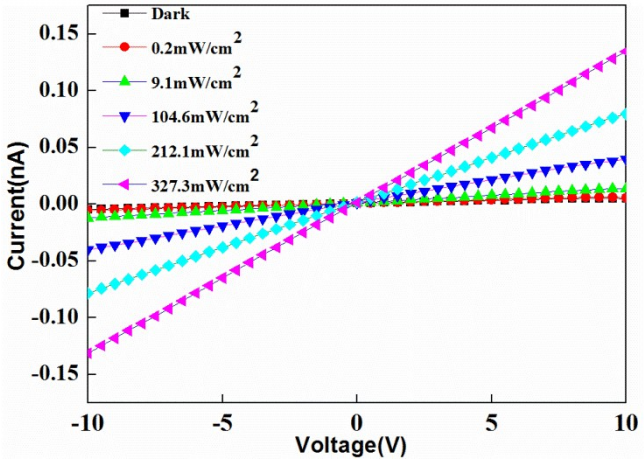

Figure S15. Variation of photocurrents with the different illuminating light power (λ = 420 nm, V_{sd} = 10 V).

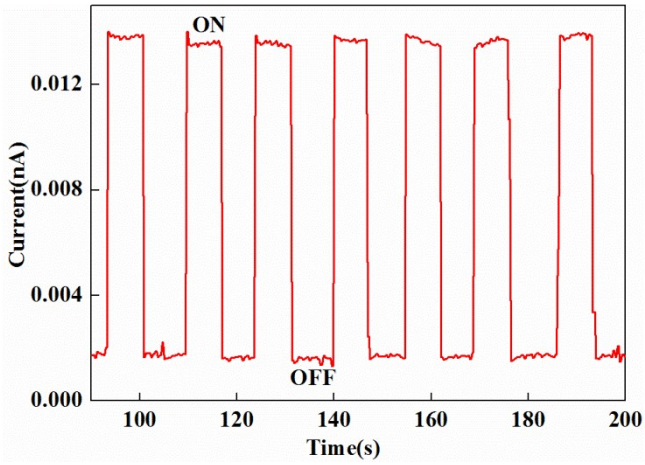

Figure S16. Recyclable switching operation of photocurrent response, showing no obvious attenuation after a long-time illumination.

Table S1. Crystal data for **1**, **2** and **3**.

Empirical formula	**1** $C_8H_{22}Bi_2I_8N_2O$	**2** $C_{16}H_{44}Bi_2I_{10}N_4O_2$	**3** $C_{48}H_{132}Bi_6I_{34}N_{12}O_6$
Formula weight	1595.43	2011.51	6540.11
Temperature/K	273.15	99.99	99.98
Crystal system	monoclinic	orthorhombic	monoclinic
Space group	$P2_1/c$	Pbca	$P2_1/c$
a/Å	10.4885(7)	15.7709(7)	20.1467(13)
b/Å	24.8912(17)	22.3276(12)	22.7942(13)
c/Å	12.3295(9)	24.5774(13)	14.9932(9)
α/°	90	90	90
β/°	113.343(2)	90	91.472(2)
γ/°	90	90	90
Volume/Å^3	2955.4(4)	8654.3(8)	6883.0(7)
Z	4	8	2
ρ_{calc}g/cm^3	3.586	3.088	3.156
μ/mm^{-1}	20.250	15.276	15.304
F(000)	2728.0	7040.0	5700.0
Radiation	MoKα (λ = 0.71073)	MoKα (λ = 0.71073)	MoKα (λ = 0.71073)
2θ range for data collection/°	4.536 to 50	4.582 to 54.986	4.422 to 50
Reflections collected	33809	69514	89520
Data/restraints/parameters	5204/0/194	9885/0/315	12087/163/494
Goodness-of-fit on F^2	1.008	1.086	1.092
Final R indexes [I>=2σ (I)]	R_1 = 0.0508, wR_2 = 0.0991	R_1 = 0.0291, wR_2 = 0.0671	R_1 = 0.0877, wR_2 = 0.2370

Table S2. Selected bond lengths (Å) and bond angles (°) for **1**.

Bond lengths	Bond Angles		
Bi1-I5- 3.0035(13)	I5-Bi1-I8 170.56(4)	I1-Bi2-I5 83.91(4)
Bi2-I2- 2.8883(15)	I5-Bi1-I8^1 82.34(3)	I1-Bi2-I8^1 91.50(4)
Bi1-I8- 3.1747(13)	I5-Bi1-I6 87.12(4)	I1-Bi2-I4 161.33(4)
Bi1-I8^1- 3.4104(13)	I5-Bi1-I4 90.11(4)	I2-Bi2-I5 101.66(4)
Bi1-I6- 3.0538(13)	I8-Bi1-I8^1 88.26(3)	I2-Bi2-I8^1 170.86(4)
Bi1-I4- 3.1200(13)	I6-Bi1-I8^1 92.82(3)	I2-Bi2-I4 91.65(4)
Bi1-I7- 2.8871(13)	I6-Bi1-I8 92.60(4)	I2-Bi2-I1 96.89(5)
Bi2-I5- 3.4807(13)	I6-Bi1-I4 175.70(4)	Bi1-I5-Bi2 83.71(3)
Bi2-I8^1- 3.4281(14)	I4-Bi1-I8 89.59(4)	Bi1-I8-Bi1^1 91.74(3)
Bi2-I4- 3.3990(13)	I4-Bi1-I8^1 83.54(3)	Bi1^1-I8-Bi2^1 78.82(3)
Bi2-I3- 2.8824(14)	I7-Bi1-I5 95.37(4)	Bi1-I8-Bi2^1 132.79(4)
Bi2-I1- 2.8910(14)	I7-Bi1-I8 94.07(4)	Bi1-I4-Bi2 83.39(3)

	I7-Bi1-I8[1] 173.96(4)	I7-Bi1-I6 92.64(4)	
	I7-Bi1-I4 90.90(4)	I8[1]-Bi2-I5 75.57(3)	
	I4-Bi2-I5 78.11(3)	I4-Bi2-I81 79.28(3)	
	I3-Bi2-I5 163.78(4)	I3-Bi2 I8[1] 88.24(4)	
	I3-Bi2-I4 98.27(4)	I3-Bi2-I1 97.62(4)	
	I3-Bi2-I2 94.21(5)		

[1] 1-X,1-Y,1-Z

Table S3. Selected bond lengths (Å) and bond angles (°) for **2**.

Bond lengths	Bond Angles		
Bi1-I6- 3.4688(5)	I5-Bi1-I6 79.602(11)	I8-Bi2-I5	88.557(13)
Bi1-I5- 3.3126(5)	I2-Bi1-I6 167.424(13)	I8-Bi2-I4	88.882(13)
Bi1-I2- 2.8769(4)	I2-Bi1-I5 89.763(12)	Bi2-I6-Bi1	80.195(11)
Bi1-I4- 3.2387(4)	I2-Bi1-I4 91.951(12)	Bi2-I5-Bi1	82.153(11)
Bi1-I1- 2.9690(4)	I2-Bi1-I1 91.785(13)	Bi1-I4-Bi2	80.838(10)
Bi1-I3- 2.9262(5)	I2-Bi1-I3 93.268(14)	I4-Bi1-I6	80.117(11)
Bi2-I6- 3.1617(4)	I4-Bi1-I5 82.570(11)	I1-Bi1-I6	95.088(11)
Bi2-I5- 3.1954(4)	I1-Bi1-I5 91.126(12)	I1-Bi1-I4	172.656(13)
Bi2-I4- 3.3565(5)	I3-Bi1-I6 96.832(13)	I3-Bi1-I5	174.565(13)
Bi2-I9- 2.9721(5)	I3-Bi1-I4 92.810(13)	I3-Bi1-I1	93.287(14)
Bi2-I7- 2.9303(5)	I6-Bi2-I5 86.173(12)	I6-Bi2-I4	82.972(11)
Bi2-I8- 3.0035(5)	I5-Bi2-I4 82.530(11)	I9-Bi2-I6	91.506(13)
	I9-Bi2-I5 177.103(14)	I9-Bi2-I4	95.476(12)
	I9-Bi2-I8 93.514(14)	I7-Bi2-I6	91.610(12)
	I7-Bi2-I5 91.874(12)	I7-Bi2-I4	172.435(13)
	I7-Bi2-I9 89.922(13)	I7-Bi2-I8	96.090(14)
	I8-Bi2-I6 170.807(14)		

Table S4. Selected bond lengths (Å) and bond angles (°) for **3**.

Bond lengths		Bond Angles			
Bi1-I4	3.284(2)	I5-Bi1-I4 81.80(6)		I14-Bi3-I13	95.35(7)
Bi1-I5	3.218(2)	I5-Bi1-I6 83.50(6)		I14-Bi3-I10	91.80(8)
Bi1-I6	3.263(2)	I6-Bi1-I4 80.60(6)		I14-Bi3-I11	89.75(7)
Bi1-I2	2.972(2)	I2-Bi1-I4 89.90(6)		Bi2-I4-Bi1	81.77(5)
Bi1-I3	2.888(2)	I2-Bi1-I5 170.10(7)		I17[1]-I18-I17	180.0
Bi1-I1	2.947(2	I2-Bi1-I6 89.85(6)		Bi1-I5-Bi2	79.03(5)
Bi2-I4	3.070(2)	I3-Bi1-I4 173.49(7)		I16[2]-I15-I16	180.0
Bi2-I5	3.322(2)	I3-Bi1-I5 93.40(7)		Bi2-I6-Bi1	80.22(6)
Bi2-I6	3.196(2)	I3-Bi1-I6 94.54(7)		Bi2-I9-Bi3	154.63(9)
Bi2-I9	3.055(2)	I3-Bi1-I2 94.44(7)		I3-Bi1-I1	93.61(7)
Bi2-I8	2.992(2)	I1-Bi1-I4 91.00(7)		I1-Bi1-I5	92.56(7)
Bi2-I7	2.918(2)	I1-Bi1-I6 171.14(7)		I1-Bi1-I2	92.97(7)
Bi3-I9	3.315(2)	I4-Bi2-I5 83.42(6)		I4-Bi2-I6	85.02(6)

Bi3-I12	3.267(2)	I6-Bi2-I5	82.90(6)	I9-Bi2-I4	167.92(7)
Bi3-I13	2.987(2)	I9-Bi2-I5	87.95(6)	I9-Bi2-I6	85.54(6)
Bi3-I10	2.965(2)	I8-Bi2-I4	91.49(6)	I8-Bi2-I5	93.56(7)
Bi3-I11	3.203(2)	I8-Bi2-I6	175.28(7)	I8-Bi2-I9	97.48(7)
Bi3-I14	2.895(3)	I7-Bi2-I4	90.64(7)	I7-Bi2-I5	171.04(7)
I18-I17[1]	2.933(2)	I7-Bi2-I6	89.94(7)	I7-Bi2-I9	96.87(7)
I18-I17	2.933(2)	I7-Bi2-I8	93.29(7)	I12-Bi3-I9	83.95(6)
I15-I16[2]	2.917(2)	I13-Bi3-I9	84.73(6)	I13-Bi3-I12	83.12(6)
I15-I16	2.917(2)	I13-Bi3-I11	169.06(7)	I10-Bi3-I9	89.21(7)
		I10-Bi3-I12	167.76(7)	I10-Bi3-I13	86.16(7)
		I10-Bi3-I11	84.01(7)	I11-Bi3-I9	90.34(6)
		I11-Bi3-I12	106.11(6)	I14-Bi3-I9	178.99(8)
		I14-Bi3-I12	95.06(7)		

[1]1-X,1-Y,-Z; [2]-X,1-Y,-Z